24th COBEM - 2017

24th ABCM International Congress of Mechanical Engineering
December 3-8, 2017, Curitiba, PR, Brazil

COBEM-2017-5951
DYNAMIC ANALYSIS OF A GEODESIC DOME

Lucas de Sant'Anna Vitor Barbieri
Nilson Barbieri
Pontifícia Universidade Católica do Paraná, Department of Mechanical Engineering, Curitiba, Brazil
lucas.barbieri@hotmail.com; nilson.barbieri@pucpr.br

Roberto Dalledone Machado
Universidade Federal do Paraná, Programa de Pós-Graduação em Métodos Numéricos em Engenharia, Curitiba, Brazil
roberto.dalledonemachado@gmail.com

Abstract. *In this work the dynamic behaviour of a geodesic dome in aluminium alloy is analyzed through numerical models obtained by the Finite Element Method and tests carried out in the laboratory. It was noted that the numerical and experimental modal results have large differences. Dynamic tests were performed using impulse excitation (impact hammer) and sweep frequency through harmonic excitation (mini-shaker) to identify the natural frequencies of the structure. Using the theory of Fourier and wavelet transform, it was possible to visualize different dynamic behaviour of joints. Possible causes for the differences involve the type of joint, the fixing of the elements in the joints, the profile adopted for the elements and boundary conditions for the numerical model.*

Keywords: *geodesic dome, vibrations, Fourier transform.*

1. INTRODUCTION

The geodesic domes are structures with a resistance/weight ratio much greater than other types of structure (Ramaswamy, 2002). Currently the use of geodesic domes is associated with large buildings. According to Bysiec (2013) the geodesic domes can be assembled to cover spans over than 300m without intermediate columns. The first Geodesic Dome built in history was in Germany in a city named as Jena (Germany) in 1922. It was a planetary built by Walter Buersfeld for Zeiss industry according to Makowski (1981). However, it is impossible speak on geodesic domes without speak on Fuller. Robert Buckminster Fuller was the bigger sponsor of Geodesic Domes, Kubic (2009). In his book, Synergetics, Explorations in the Geometry of Thinking (1975), wrote about safe energy and develop a world that consume less energy. Fuller classified Geodesic Dome as a special type of Tensegrity Structures, what he considered a bigger group of structures. The name Tensegrity is the contraction between two words "Tensional" and "Integrity". Kenner (1976) and Clinton (1965) demonstrated the math to find the coordinates of the nodes that will generate the geodesic dome. They also classified the geodesic domes according to method is used to find the coordinates. The oil industry has used geodesic dome to cover storage tanks because geodesic domes has helped to avoid evaporation from the storage product and rain water contamination. The geodesic dome do not need intermediate columns to cover the tank so it allows an increase in efficiency of the internal floating roof. For more details, see Rossot (2014) and Giacomitti *et al*., (2015). In this work a physical model based on a real structure was built. The physical model was submitted to dynamic tests. The Frequency Response Function (FRF) and the Wavelet transform were used to investigate dynamic behaviour of the joints.

2. PHYSICAL MODEL DESIGN

The physical model was based in a real structure used to cover a gasoline tank with 24 m diameter. The geodesic dome used to cover the gasoline tank is illustrated in Fig. 1. Details about the design as, cross section of the bars, size and coordinates of the nodes, are according to Rossot (2014). In Fig. 2 are shown the pieces that were used to set the physical model. In Fig. 3a is illustrated the physical model already built. Figure 3b show a detail of a node. Since the aim of this paper is to study the structure of the geodesic dome and the panels used to cover the real geodesic dome are very thin, they was not erected on the physical model.

Figure 1. Geodesic dome used to cover a tank with 24m diameter

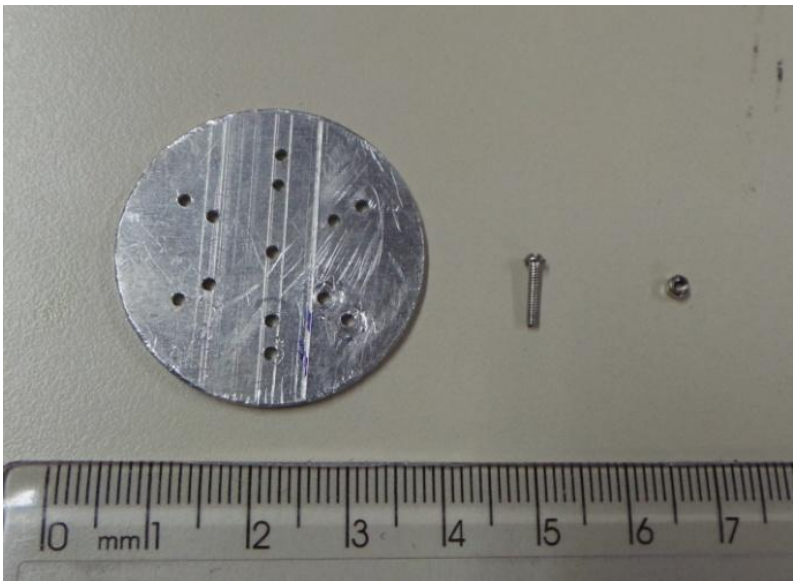

Figure 2. Demonstration of the scale of the model

Figure 3. Physical model already built (a) and detail of a node (b)

The structure is composed of 130 beams and 51 joints (Fig. 4). The beams (L profile) were divided into 15 types (B1 to B15) (Tab. 1) varying according to the length. Note that the structure pattern is repeatable at every 72 ° (Fig. 5).

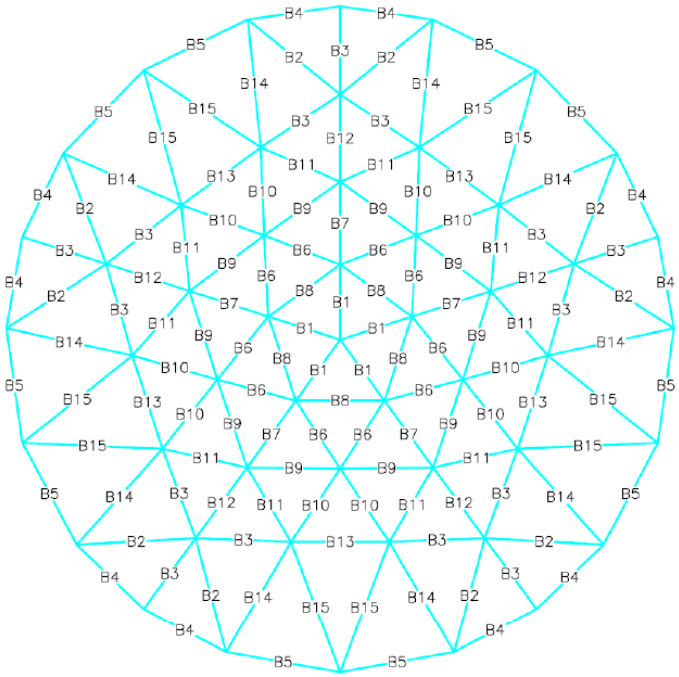

Figure 4. Representation of the beams in the structure

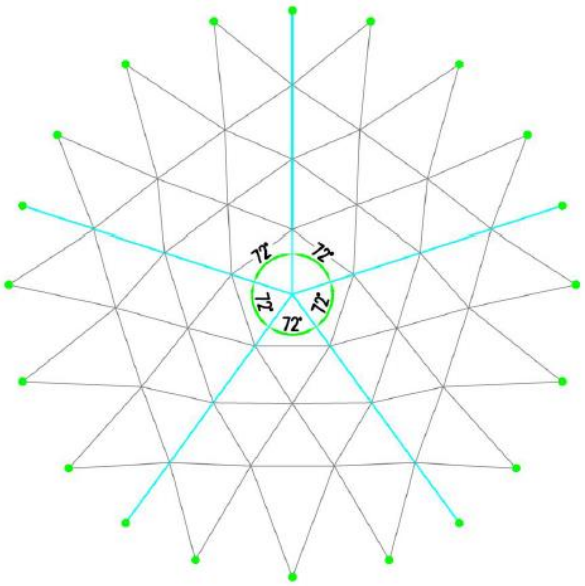

Figure 5. Model symmetry

Table 1. Size and number of beams in the structure.

Bar	Lpt(mm)	Quantity
B1	227.93	5
B2	377.80	10
B3	290.75	15
B4	281.14	10
B5	349.40	10
B6	246.44	10
B7	253.51	5
B8	267.58	5
B9	281.40	10
B10	272.90	10
B11	264.30	10
B12	275.58	5
B13	296.19	5
B14	418.80	10
B15	450.82	10
	Total	130

3. DYNAMIC TEST

Dynamic test were performed in the laboratory to obtain the modal parameters. The first dynamic test was carried out using an impact hammer for the system excitation and vibratory data were obtained from six accelerometers placed on the structure (Fig. 6). The specification of the impact hammer and accelerometers are shown in Tab. 2.

Table 2. Specification of the impact hammer and accelerometers.

Description	Model	Sensitivity
Impact hammer	086C03-PCB	2.13mV/N
Accelerometer 1	333B-PCB	107,9 mV/g
Accelerometer 2	333B-PCB	109,2 mV/g
Accelerometer 3	333B-PCB	111,8 mV/g
Accelerometer 4	333B-PCB	111,5 mV/g
Accelerometer 5	333B-PCB	101,1 mV/g
Accelerometer 6	333B-PCB	109,9 mV/g

The basic idea of this paper is to obtain Function Frequency Response FRF of the structure. This parameter is the most used for modal identification of structures. Through the analysis of the curves, it is possible to identify energy concentration regions associated with the natural frequencies of the system. In a further analysis, the inverse of the FRF signals were converted for the time domain to the use of wavelet theory. The goal was to identify energy concentration regions using the joint vibration signals. Figure 7 shows the force and Fig. 8 the acceleration signals in time domain. In this case was used four impulsive force to obtain the average of the signals. Figure 9 shows the FRF curve of one accelerometer and Fig. 10 the correspondent IFRF curves. It can be noted in Fig. 9 that there is a region of energy concentration near to frequency band of 30 Hz. This frequency of resonance is not present in the numerical results, where the first natural frequency is around 200 Hz order.

Figure 6. Impulsive test using impact hammer

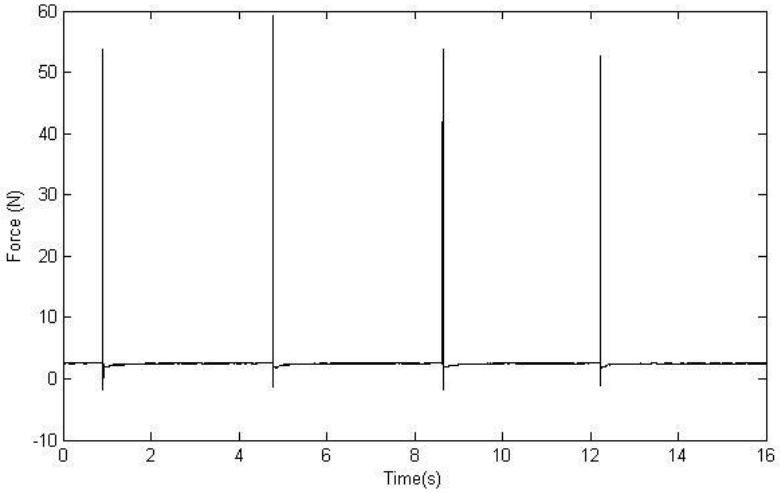

Figure 7. Impulsive force

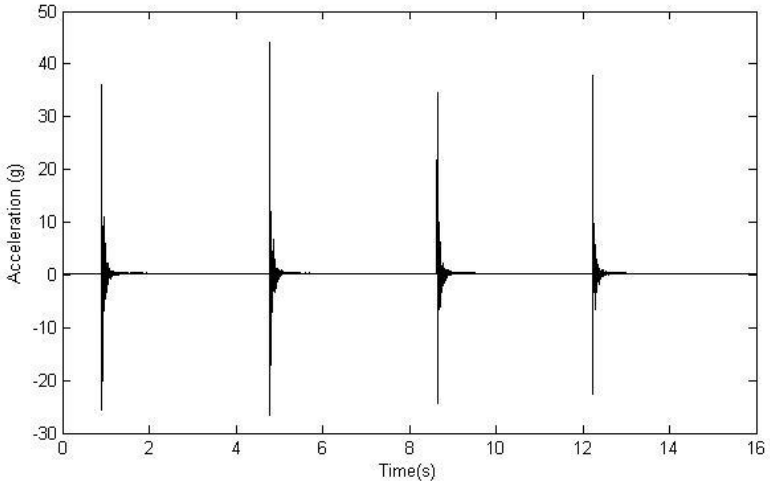

Figure 8. Acceleration signal

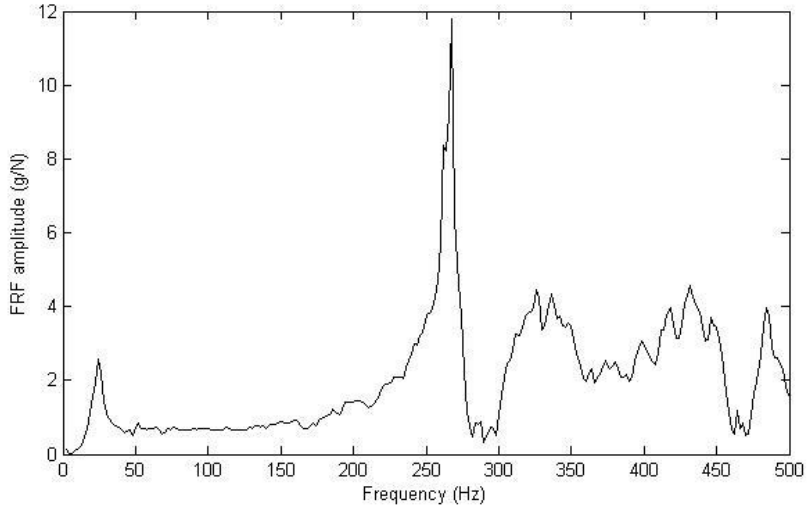

Figure 9. FRF curve

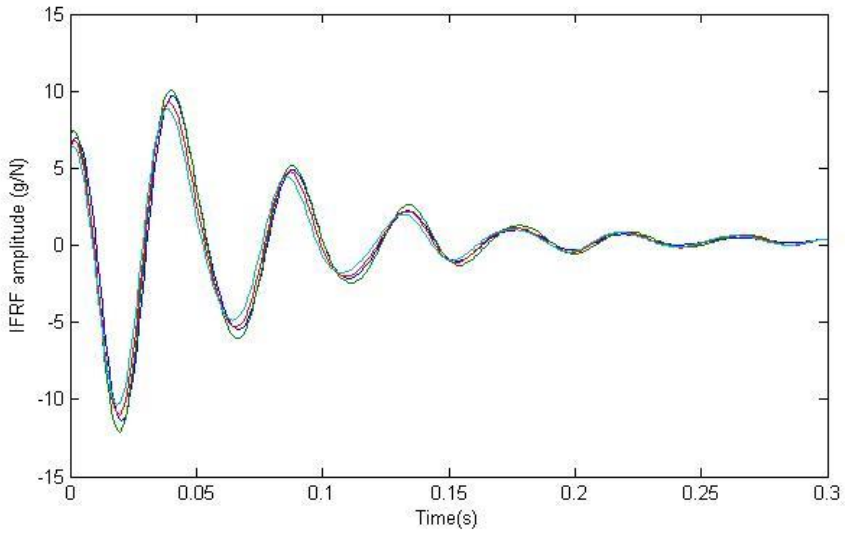

Figure 10. IFRF curve

The continuous wavelet transform (CWT) is defined in equations Eq. (1) and in Eq. (2) (Qin *et al*., 2015). ψ is a window function called the mother wavelet, where *a* is a scale and *b* is a translation. An energy index based on Eq. (2) was used to analyze de dynamic behavior of the joints. In this case, the analyzed signal was the inverse of the FRF. Figure 11 shows two different curves of energy for two different joints (symmetrical in the model).

$$C(a,b) = \int_{-\infty}^{+\infty} f(t)\,\psi_{a,b}(t)dt \tag{1}$$

$$\psi_{a,b}(t) = a^{1/2}\psi\left(\frac{t-b}{a}\right) \tag{2}$$

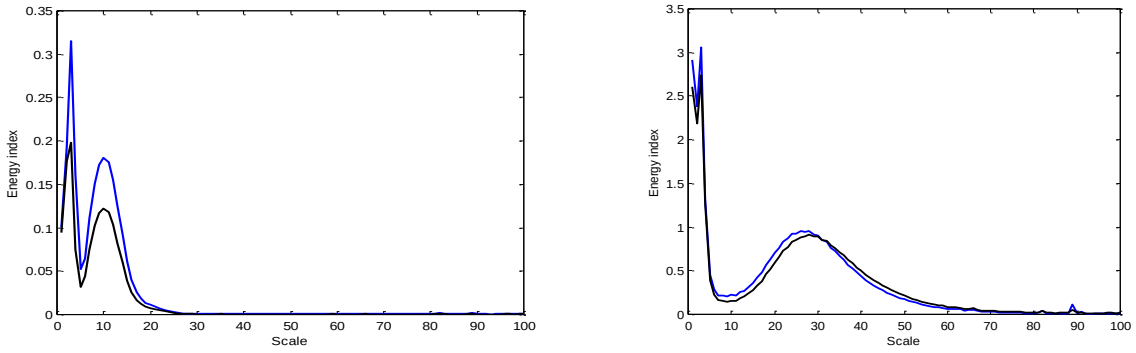

Figure 11. Energy curves of two different joints using wavelet transform

It is evident from the figures that there are large differences in signal behavior in the joints. These energy concentration regions are related to different resonance frequencies of the system.

Figure 9 shows the FRF curve for the accelerometer located at node 31. It is noted a region of energy concentration around 25 Hz. From this information, through digital filtering in the range of 10 to 30 Hz, the inverse of FRF was obtained. The wavelet transform was applied to the filtered signal and the energy curves are shown in Fig. 12.

The wavelet transform allows the signal decomposition as a function of time (by translation) and in scale (by dilation or contraction) instead analysis in time and frequency domain as in the case of Fourier Transforms. The time-scale analysis enables detail locally, the information on a sign. Moreover, do not require for the representation of a function, a large amount of coefficients, as is the case of the Fourier Transform. A detailed description of the wavelet transform can be found at Daubechies (1999), Rucka and Wilde (2006) and Lima *et al*., (2015).

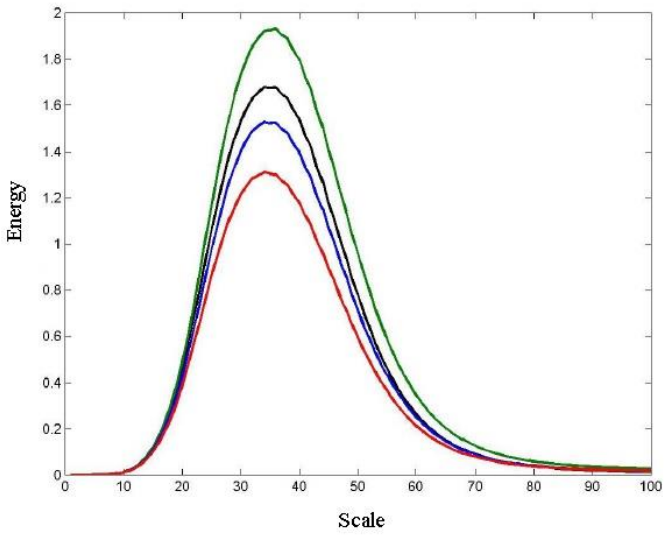

Figure 12. Wavelet transform applied to a filtered signal

The second dynamic test was carried out using a mini-shaker for the system excitation (Fig. 13) and vibratory data were obtained from six accelerometers placed on the structure. The mini-shaker used was a Bruel & Kjaer, model 4810, coupled with a power amplifier, Bruel & Kjaer, model 2706. To measure the force, a Bruel & Kjaer impedance head, model 8001, sensitivity of 379 mV/N and a Bruel & Kjaer signal amplifier, model 2525, were used. The test was performed by varying the excitation frequency from 10 to 100 Hz, with 1 Hz increase. The results are shown in Fig. 14.

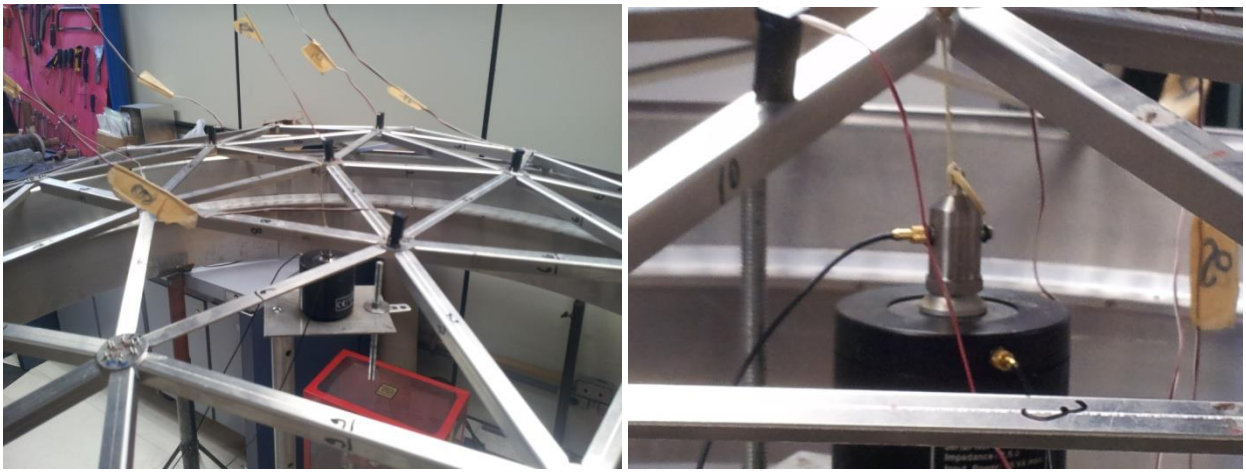

Figure 13. Dynamic test using a mini-shaker

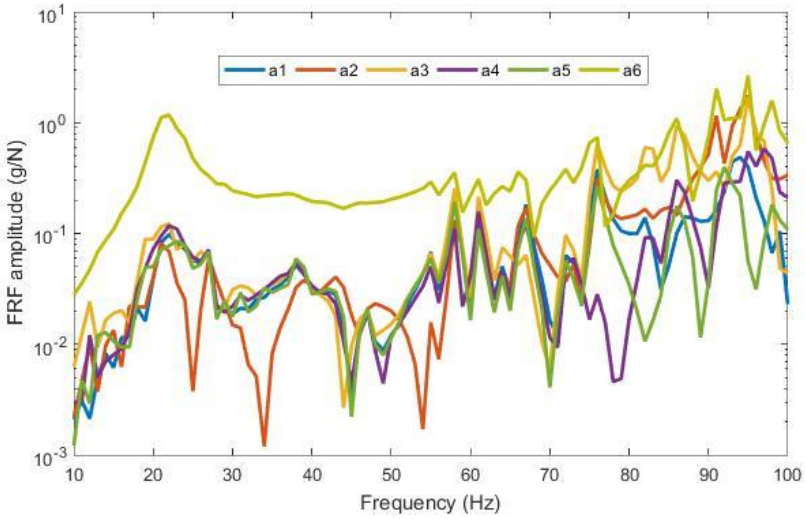

Figure 14. FRF curve of the mini-shaker test

Static tests were performed in the laboratory to measure the displacement of the joints 52, 26, 28 and 31 of the structure. The application of the loads was done in a gradual way, with the addition of weights calibrated from 2N to the maximum of 8N. To measure the displacement, a Mitutoyo dial indicator, model 7010SN, with 0.01mm resolution, was used (Fig. 15). The points of application of the load were the same points of the displacement measurement. Figure 16 shows results of the displacements in the four tested nodes.

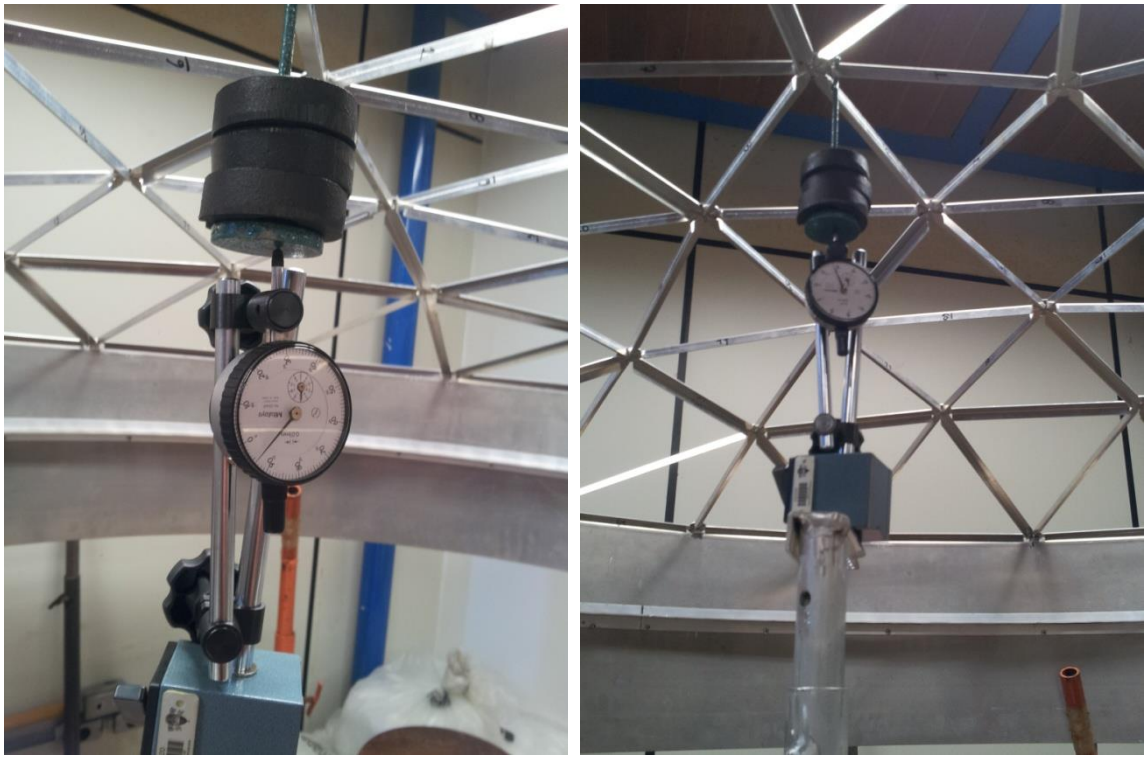

Figure 15. Static test

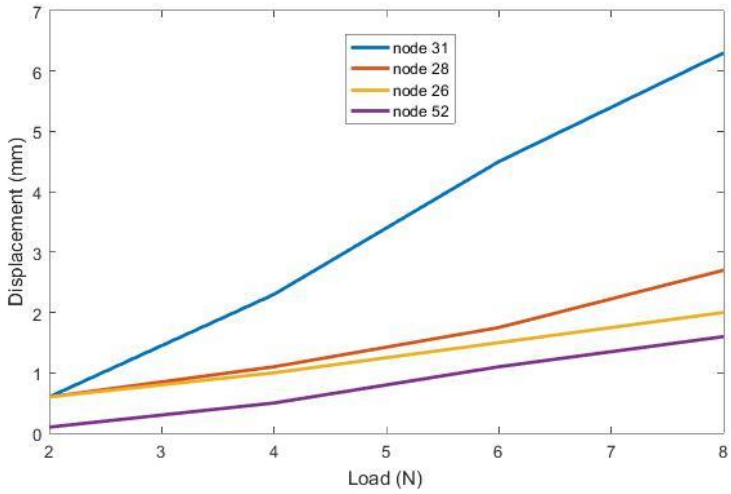

Figure 16. Static test results

4. CONCLUSIONS

Dynamic tests using two different techniques, i.e., force impulsive (impact hammer) and sweep sine excitation using a mini-shaker were performed. The signals obtained from accelerometers and impedance head were treated in Matlab to obtain the curves of Function Frequency Response. All curves were evidenced energy concentration regions to low frequencies between 25 and 100 Hz. These frequencies were not contained in the numerical results. The results of the dynamic test using the mini-shaker were not so good. Only the accelerometer 6 showed an energy concentration region near to 25Hz.The lowest rate was around 25 Hz (first vibrate mode). In an attempt to identify possible joints (nodes) that had different behaviors used an energy parameter based on wavelet transform. Doing a sweep of the major joints, it was noticed a large different behavior for one joint.

The static tests results shows that three nodes had similar behavior, however, the node 31 had a displacement much higher than the other nodes. Visually it was verified that this joint presented a large displacement by applying a small extern force, due to snap-through buckling.

Several factors may have influenced this difference in numeric and experimental values of the natural frequencies. These factors may be related to the way of fixing elements (circular piece and screws that may have gaps); the type of element used (L beam) that for fixing it was necessary to decrease the contact area; the properties of the material (aluminum alloy); the boundary conditions used in the numerical model (the elements of the ends are fixed on a circular structure that was not considered in the numerical model).

5. REFERENCES

Bysiec D., 2011. *The Investigation of Stability of Double-Layer Octahedron-Based Geodesic Domes*. Structure Environment, 3 (3), 30-41.

Clinton J., 1965. *Structural Design Concepts for future Space Missions, Progress Report* – NASA REPORT.

Daubechies, I., 1999. *The Wavelet Transform, Time-Frequency Localization and Signal Analysis*, IEEE, Transactions on Information Theory, 36 (5), 961-1005.

Fuller, R. B., 1975. *Synergetics, explorations in the geometry of thinking*. Macmillan Publishing, USA.

Giacomitti, M. R., Machado, R. D., Abdalla, J. E., 2015 *Numerical Analysis an Aluminum Geodesic Dome Roof Using the Finite Element Method*. |23rd ABCM International Congress of Mechanical Engineering. December 6-11, Brazil.

Kenner, H., 1976. *Geodesic Math and how to use it*. California, CA, USA: University of California Press.

Kubic, M., 2009. *Structural Analysis of Geodesic Domes. Durham University School of Engineering*. Final Year Project.

Lima, K. F., Barbieri, N., Barbieri, R., Winniques, L. C., 2015. *Young's Modulus and Loss Factor Estimation of Sandwich Beam with Three Optimization Methods by FEM*. International Journal of Computer Applications, 128 (3), 35-43.

Makowski, Z. S., 1981. *Analysis, Design and Construction of Double-Layer Grids*. CRC Press.

Newland D. E., 1996. *An Introduction to Random Vibrations, Spectral & Wavelet Analysis*, Published by Prentice Hall, London.

Qin, J., Sun, P., Walker, J., 2015. *A waveform profile-based noise measurement system and methodology for complex noise evaluation*. Noise Control Engineering Journal, 63 (9), 563-571.

Ramaswamy G. S., 2002. *Analysis, design and construction of steel space frames*. London: Thomas Telford.

Rossot, D., 2014. *Domos Geodésicos - Abordagem Numérica e Experimental em um Modelo Físico*. Master Dissertation. Pontificia Universidade Católica do Paraná.

Rucka M., Wilde, K., 2006. *Application of continuous wavelet transform in vibration based damage detection method for beams and plates*. Journal of Sound and Vibration, 297, (3-5), 536-560.

6. RESPONSIBILITY NOTICE

The authors are the only responsible for the printed material included in this paper.